Thermal detection of plumes produced by industrial accidents in urban areas based on the presence of the heat island

N. CHRYSOULAKIS*

Foundation for Research and Technology – Hellas, Institute of Applied Mathematics, Regional Analysis Division, IACM–FORTH, Vassilika Vouton, P.O. Box 1527, GR 71110, Heraklion, Crete, Greece;
e-mail: zedd2@iacm.forth.gr

and C. CARTALIS

University of Athens, Dept. of Applied Physics, Building PHYS-V, Athens, GR 15784, Greece. e-mail: ckartali@cc.uoa.gr

(*Received 19 March 2001; in final form 6 November 2001*)

Abstract. Detection of plumes produced by industrial accidents using NOAA/AVHRR thermal imagery may be substantially supported in urban areas by the presence of the heat island phenomenon. In this study, an attempt is made to classify the urban web on the basis of the heat island and its impact on the brightness temperatures. Application of the classification scheme on a night-time thermal infrared NOAA-14 image depicting the urban web of Athens demonstrates the potential of this classification for the detection of a plume caused by a fire in a warehouse. Detection of the plume in this case is favoured by the urban heat island phenomenon due to which the urban surface has higher temperature compared to the adjacent environment and the plume above. As a result, distinction of the pixels corresponding to the plume is more effective.

1. Introduction

In recent years, and due to a number of incidents involving fires in industrial installations and warehouses, research has focused on the definition of the properties of produced plumes. The difference between the temperature of the top of a plume and the temperature of the adjacent environment must be above a certain value for a plume to be detectable (Chung and Le 1984, Scorer 1987). This temperature difference can be estimated using thermal infrared images of the Advanced Very High Resolution Radiometer (AVHRR) on board the National Oceanic and Atmospheric Administration (NOAA) satellites.

Detection of a plume is favoured by the urban heat island phenomenon due to the fact that the urban surface has higher temperature than the adjacent environment and the plume above. As a result pixels that correspond to the land surface present strong temperature differences to the pixels corresponding to the top of the plume.

* Author for correspondence

International Journal of Remote Sensing
ISSN 0143-1161 print/ISSN 1366-5901 online © 2002 Taylor & Francis Ltd
http://www.tandf.co.uk/journals
DOI: 10.1080/01431160110111973

This fact allows the plume to be more easily detected in the thermal infrared when the plume is diffused over a city than when it is diffused over a suburban region.

In this study, an attempt was made to develop a classification scheme for urban areas on the basis of the heat island and its impact on brightness temperatures. The scheme was used to display a plume that was caused by a fire in the installations of a Navy warehouse shop in Iera Odos, Votanikos in the city of Athens. This display was based on the distinction of the pixels corresponding to the top of the plume from those corresponding to the surface of the urban web below, using the AVHRR Channel 4 (10.3–11.3 μ) Brightness Temperature (hereinafter referred to as BT_4) differences. For this reason, the distribution of BT_4 must be estimated for the broader Athens area.

2. Data and methodology

For the purposes of this study, four high spatial resolution NOAA AVHRR images (Local Area Coverage) were used as acquired from the Dundee University and the University of the Aegean satellite stations. All images were night-time (01:44 UTC). Three of the images were taken from NOAA-14 during the period 15–17 July 1998. These dates were selected in order to estimate the intensity of the heat island phenomenon over the city of Athens, at a time when a high-pressure system was located over Greece. It should be mentioned that the heat island is favoured by high-pressure systems and cloud free conditions, especially in summer. The fourth image was taken from NOAA-14 on 7 March 1998. This date was selected because at 20:30 Local Time a fire developed in the installations of a Navy warehouse shop in Iera Odos, Votanikos in the city of Athens. The fire spread quickly destroying the food and clothing departments and there also was a human casualty. In figure 1 the black spot delimits the area under investigation.

AVHRR has a spatial resolution of 1.1 km at nadir. The images used are in NOAA Level 1-b format and they are structured in 10-bit (1024 grey level) words. Initially AVHRR images were geometrically corrected using the information (Ground Control Points) embedded in Level 1-b format. Following the geometric correction, a common projection system was used for all AVHRR images, as well as for the map of the broader Athens area. At the next stage, AVHRR images were calibrated, in order to transform grey level values (raw counts or digital numbers) to brightness temperature values for each pixel of infrared channels.

For the purposes of this study, the spatial distribution of AVHRR channel 4 brightness temperature (BT_4) for the broader Athens area was defined. To this end digital numbers were converted to at-sensor spectral radiances for channel 4, using equation 1 (Kidwell 1997):

$$L_4 = A_{4(j)}DN + B_{4(j)} \tag{1}$$

where DN is the digital number for channel 4, for each pixel. DN varies from 0 to 1023 counts; $A_{4(j)}$ is the slope for channel 4 for satellite scan line (j) (mW m^{-2} sr^{-1} cm); $B_{4(j)}$ is the intercept value for channel 4 for satellite scan line (j) (mW m^{-2} sr^{-1} cm); and L_4 is the spectral radiance for channel 4, for each pixel (mW m^{-2} sr^{-1} cm).

$A_{4(j)}$ and $B_{4(j)}$ were derived from radiometric in-flight calibration following the NOAA-NESDIS procedure which is based on regular measurements of deep space and the AVHRR internal blackbody temperature. $A_{4(j)}$ and $B_{4(j)}$ were embedded in Level 1-b format and allowed the linear calibration of AVHRR channel 4 using equation 1. These coefficients provide a linear radiance (L_4); consequently a non-linearity correction for channel 4 should be applied. The corrected radiance for

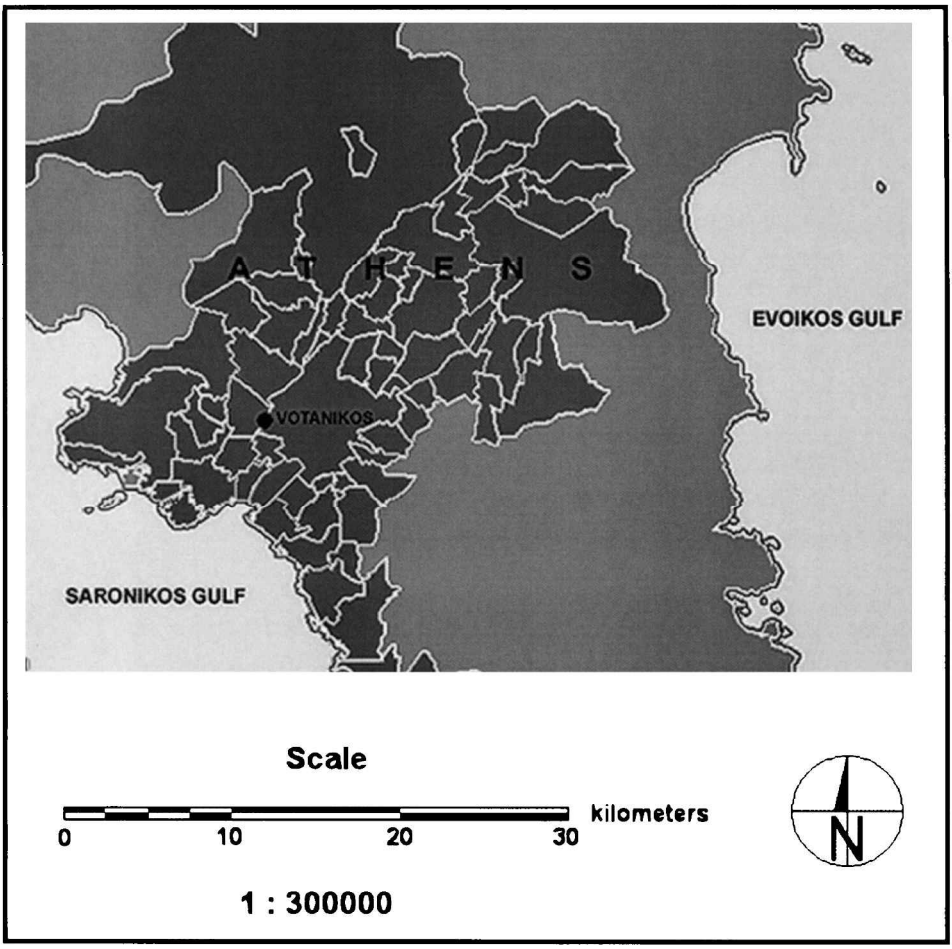

Figure 1. Map of the broader Athens area. The urban web is shown by the dark grey colour. The black spot delimits the site of the industrial accident (Iera Odos, Votanikos).

channel 4 (RAD_4) is calculated from L_4 values using equation 2 (Kidwell 1997):

$$RAD_4 = 0.92378(L_4) + 0.0003822(L_4)^2 + 3.72 \quad (2)$$

RAD_4 can be converted to brightness temperature (BT_4) for each pixel using the inverse of the Plank function with the appropriate central wave number. Therefore, BT_4 can be calculated using equation 3 (Kidwell 1997):

$$BT_4 = \frac{C_2 v_4}{\ln\left[1 + \left(\frac{C_1}{RAD_4}\right) v_4^3\right]} \quad (3)$$

where BT_4 is the brightness temperature for channel 4, for each pixel (K); RAD_4 is the corrected spectral radiance for channel 4, for each pixel ($mW\,m^{-2}\,sr^{-1}\,cm$); C_1 is the constant $1.1910659 \times 10^{-5}\,mW\,m^{-2}\,sr^{-1}\,cm^4$; C_2 is the constant $1.438833 \times 10^{-5}\,cm\,K$; and v_4 is the central wave number for channel 4 (cm^{-1}). In

this study, we have considered that the surface temperature should be between 270 K and 310 K. According to Kidwell (1997) v_4 must have the value 929.3323 cm^{-1}.

The aforementioned calibration method has been developed by NOAA-NESDIS in order to provide prelaunch information to operational data users, that is both concise and accurate. It corrects the linear radiance estimate instead of correcting equivalent blackbody temperature values. The error in calculating brightness temperature values was within 0.1–0.2 K for channel 4 (Sullivan 1999).

Subsequently, a supervised classification was performed in all AVHRR channel 4 images. BT_4 values of each pixel were distributed in six classes. In order to define these classes, the mean BT_4 value was calculated for the pixels representing the urban web. The relative positions of these pixels on the channel 4 image were related to the map of the broader Athens area (figure 1). The name and the definition of each class are presented in table 1.

The above classification scheme, which is in practice a simple thresholding procedure, was selected to classify the pixels according to their temperature difference from T_0. The width of each class (with the exception of the first class and the last one) is 1 K. Given that the brightness temperature differences between pixels corresponding to the top of the plume and pixels corresponding to the urban web are greater than 1 K (and are enhanced at the presence of the heat island), a distinction of the pixels is allowed since they are included in different classes. Applying the thresholding procedure in every AVHRR channel 4 image, a new thematic image is produced. Different colours are used to display each class on the thematic images.

3. Results

Figures 2(a) and 2(b) present the spatial distribution of BT_4 (for $T_0 = 296$ K and 295 K respectively) resulting from the classification of the AVHRR channel 4 brightness temperature images of 15 July 1998 and 16 July 1998. The heat island phenomenon is evident in both cases. The pixels corresponding to areas that have been affected by the heat island phenomenon are included in the second class (displayed with red colour). According to the map of figure 1, these pixels represent the centre of the city and the area around it. In the same area, some pixels are displayed in blue (third class). This implies that these pixels have BT_4 which is 1 K less than T_0 and are representative of the industrial area of Athens, which is located near the centre of the city.

Figure 2(c) presents the spatial distribution of BT_4 (for $T_0 = 293$ K) resulting from the classification of the AVHRR channel 4 brightness temperature image of 17 July 1998. The heat island phenomenon is more evident in this case. The pixels

Table 1. Definition of the six classes that were used in the supervised classification scheme. BT_4 value of each pixel defines the respective class. T_0 is the mean BT_4 value for the pixels representing the urban web.

Class name	Class definition
$> T_0$	$BT_4 \geqslant T_0 + 0.5$ K
T_0	$T_0 - 0.5$ K $\leqslant BT_4 < T_0 + 0.5$ K
$T_0 - 1$	$(T_0 - 1) - 0.5$ K $\leqslant BT_4 < (T_0 - 1) + 0.5$ K
$T_0 - 2$	$(T_0 - 2) - 0.5$ K $\leqslant BT_4 < (T_0 - 2) + 0.5$ K
$T_0 - 3$	$(T_0 - 3) - 0.5$ K $\leqslant BT_4 < (T_0 - 3) + 0.5$ K
$< T_0 - 3$	$BT_4 < (T_0 - 3) - 0.5$ K

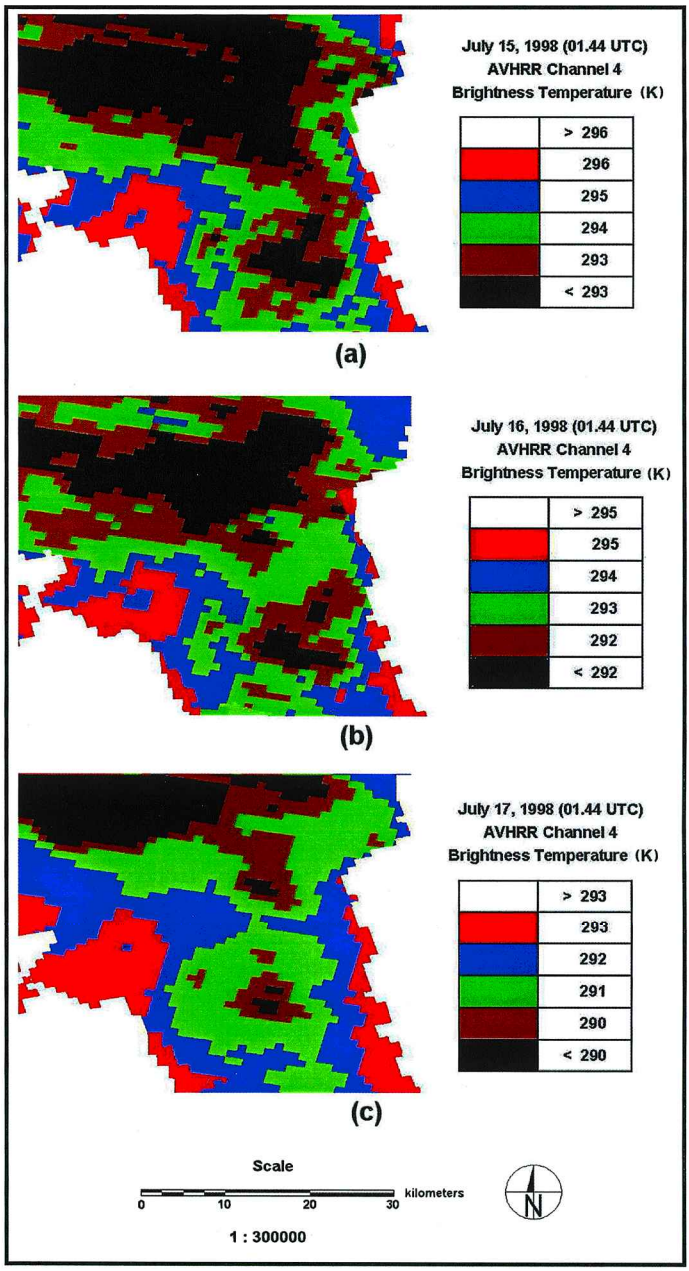

Figure 2. Thematic images of the broader Athens area resulting from the classification of the AVHRR channel 4 brightness temperature images of (a) 15, (b) 16 and (c) 17 July 1998 (01.44 UTC). The spatial distribution of BT_4 is shown using six distinct classes.

corresponding to areas that have been affected by the heat island phenomenon are included in the second class (displayed with red colour). According to the map of figure 1(a), these pixels represent the greater part of the city around its centre.

In the above cases, the difference in BT_4 between the centre of the city and the

suburban areas (magnitude of the heat island) is about 2–3 K and it is in accordance to Katsoulis and Theoharatos (1985).

Figure 3(a) presents the spatial distribution of BT_4 (for $T_0 = 280$ K) resulting from the classification of the AVHRR channel 4 brightness temperature image of 7 March 1998. For better display, pixels which have T_0 of $0.5\,K \leqslant BT_4 < T_0 + 0.5\,K$ are displayed with blue colour; these pixels correspond to areas which have been affected by the heat island phenomenon. The second class, in this case, includes pixels representing the coastal area of Athens. At this time of year, the coastal line has greater temperatures than the centre of the city (see Katsoulis and Theoharatos 1985).

An area in brown appears in the urban web, where only blue or green colours are expected due to the heat island phenomenon; the corresponding pixels of this area belong to the fifth class. This implies that lower brightness temperatures (by approximately 2 K) are observed in this area, which lies over the accident site. This may be verified by creating a digital mask for this (T-shaped) area and by applying the mask to the map of the broader Athens area. As shown in figure 3(b), the relative position of the mask on the map is over Iera Odos, Votanikos, which is the accident site. It should be mentioned that all images and the map are in the same projection system.

The assignment of the pixels to the fifth class can be explained from the presence of the plume over the accident area. Practically, this implies that the pixels for which the brightness temperature is estimated corresponds to the top of the plume. As a result, the thermal detection of the pixels corresponding to the plume is favoured by the heat island phenomenon, due to which a brightness temperature difference greater than 1 K appears, between the pixels corresponding to the top of the plume and the pixels corresponding to the urban background. If the site of the accident was in the suburban area, the thermal detection of the plume should be unattainable, because the pixels corresponding to the top of the plume, as well as the pixels corresponding to the suburban background, should be included in the same class (fifth) and should be displayed in the same colour (brown).

4. Conclusions

The temperature difference of a plume to its surroundings is typical over the urban web of a large city at night. Due to the urban heat island phenomenon, pixels corresponding to the land surface obtain traceable temperature differences to pixels corresponding to the top of the plume. This makes the plume more distinct in the thermal infrared when diffused over a city, than when diffused over a rural or suburban area.

The methodology used to assess this temperature difference between the plume and the surface was based on an analysis of the distribution of the brightness temperature difference in AVHRR channel 4. Brightness temperatures (BT_4) were calculated by transforming grey level values in brightness temperature values for each pixel of the geometrically corrected AVHRR channel 4 image. A supervised classification was performed and the BT_4 values were distributed in six classes. These classes were defined using the mean BT_4 value for the pixels representing the urban web.

Using this method, the plume resulting from a fire in the installation of the Navy warehouse shop in the city of Athens in the Votanikos area was detected. The thermal detection of the plume was achieved because the pixels corresponding to the top of the plume and the pixels corresponding to the urban background reflected

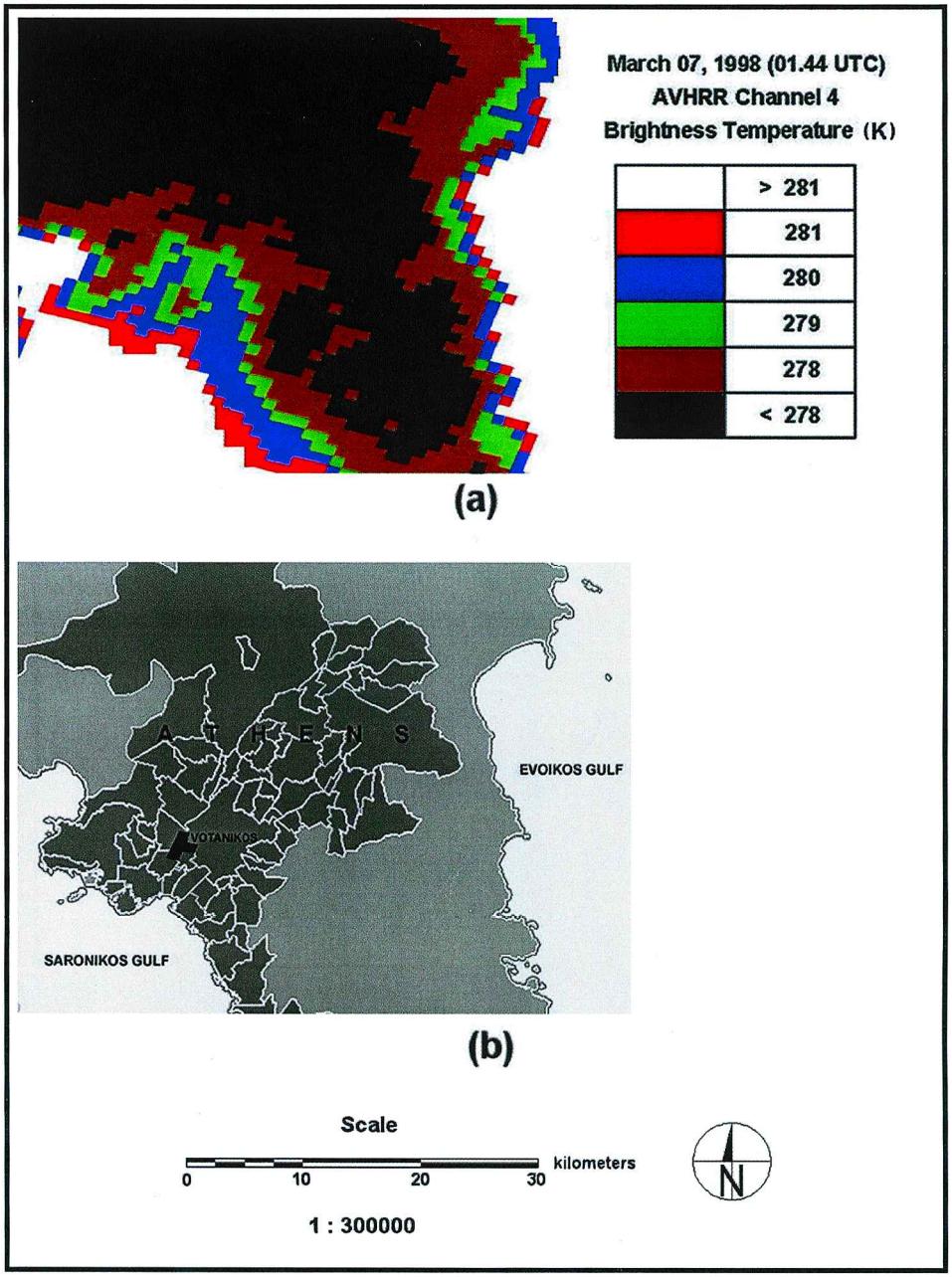

Figure 3. (a) Thematic image of the broader Athens area as a result of the classification of the AVHRR channel 4 brightness temperature image of 7 March 1998 (01.44 UTC). The spatial distribution of BT_4 is shown using six distinct classes. An area in brown appears in the urban web, where only blue or green colours should be expected due to the heat island phenomenon. This area practically refers to the area covered by the plume produced by an industrial accident. (b) Map of the broader Athens area, following the application of the digital mask (T-shape black area). This digital mask has been developed using the pixels which correspond to the plume area detected in (a). The relative position of the mask on the map, is over Iera Odos, Votanikos, which is the accident site.

different classes and could thus be easily separated. In particular, lower brightness temperatures (by as much as 2 K) correspond to pixels representing the top of the plume.

References

CHUNG, Y. S., and LE, H. V., 1984, Detection of forest-fire smoke plumes by satellite imagery. *Atmospheric Environment*, **18**, 2143–2151.

KATSOULIS, B. D., and THEOHARATOS, G. A., 1985, Indications of the urban heat island in Athens. *Journal of Climate and Applied Meteorology*, **24**, 1296–1302.

KIDWELL, K. B. (editor), 1997, *NOAA polar orbiter data users guide*. (Washington, DC: US Department of Commerce, National Oceanic and Atmospheric Administration).

SCORER, R. S., 1987, Hot Spots and Plumes: Observation By Meteorologiacal Satellites. *Atmospheric Environment*, **21**, 1427–1435.

SULLIVAN, J., 1999, New radiance-based method for AVHRR thermal channel nonlinearity corrections. *International Journal of Remote Sensing*, **20**, 3493–3501.